NASA Contractor Report 198169

ICASE Report No. 95-44

ICASE

ANALYSIS AND MODELING OF SUBGRID SCALAR MIXING USING NUMERICAL DATA

Sharath S. Girimaji
Ye Zhou

Contract No. NAS1-19480
May 1995

Institute for Computer Applications in Science and Engineering
NASA Langley Research Center
Hampton, VA 23681-0001

Operated by Universities Space Research Association

Analysis and modeling of subgrid scalar mixing using numerical data*

Sharath S. Girimaji and Ye Zhou

Institute for Computer Applications in Science and Engineering

NASA Langley Research Center, Hampton, VA 23681

Abstract

Direct numerical simulations (DNS) of passive scalar mixing in isotropic turbulence is used to study, analyze and, subsequently, model the role of small (subgrid) scales in the mixing process. In particular, we attempt to model the dissipation of the large scale (supergrid) scalar fluctuations caused by the subgrid scales by decomposing it into two parts: (i) the effect due to the interaction among the subgrid scales, $\mathcal{E}_\phi^{>>}$; and, (ii) the effect due to interaction between the supergrid and the subgrid scales, $\mathcal{E}_\phi^{><}$. Model comparison with DNS data shows good agreement. This model is expected to be useful in the large eddy simulations of scalar mixing and reaction.

*This research was supported by the National Aeronautics and Space Administration under NASA Contract No. NAS1- 19480 while the authors were in residence at the Institute for Computer Applications in Science and Engineering (ICASE), NASA Langley Research Center, Hampton, VA 23681-0001.

1 Introduction.

Large eddy simulation (LES) of turbulent mixing and reaction is a possible means of calculating complex flows not amenable to the full direct numerical simulations (DNS) [1], [2]. In performing the LES of combustion, one is faced with a modeling problem not present in the LES of Navier-Stokes equation, that of molecular mixing of scalars. Many combustion problems of practical interest are of the non-premixed type. In non-premixed combustion, scalar mixing, to a large extent, controls the rate of reactant conversion. Scalar mixing is predominantly a small-scale phenomenon occurring in scales not resolved in LES calculations. Adequate modeling of the subgrid-scale mixing process is, hence, crucial to the success of LES of reacting flows.

Consider the mixing and reaction of a scalar field $\phi(\mathbf{x},\mathbf{t})$ in an incompressible turbulent velocity field $\mathbf{u}(\mathbf{x},\mathbf{t})$:

$$\frac{\partial \phi}{\partial t} + u_a \frac{\partial \phi}{\partial x_a} = \mu_0 \frac{\partial^2 \phi}{\partial x_a \partial x_a} + w(\phi), \tag{1}$$

where μ_0 and w are the molecular diffusivity and the chemical conversion rate of the scalar. (Repeated indices imply summation.) In a turbulent flow, u_a and ϕ fields are made up of the entire gamut of scales ranging from the energy containing scales to the dissipative scales. In a high Reynolds number flow of complex geometry, a DNS calculation that resolves all of the length and time scales represents a formidable task. Large eddy simulation entails the calculation of the energy containing (called supergrid or resolved) scales only. The dissipative and dispersive action of the small (called subgrid or unresolved) scales on the large scales are accounted for by using suitable models.

The resolved field of any quantity $\overline{A}$ is obtained from its full field A by employing a filter G of specified width Δ:

$$\overline{A(\mathbf{x},t)} = \int_{-\infty}^{\infty} A(\mathbf{x}',t) G(\mathbf{x}-\mathbf{x}',\Delta) d^3x'. \tag{2}$$

The unresolved field, A', is given by

$$A'(\mathbf{x},t) = A(\mathbf{x},t) - \overline{A(\mathbf{x},t)}. \tag{3}$$

When the filter is applied to the scalar evolution equation (1) we get

$$\frac{\partial \overline{\phi}}{\partial t} + \overline{u_a}\frac{\partial \overline{\phi}}{\partial x_a} = \mu_0 \frac{\partial^2 \overline{\phi}}{\partial x_a \partial x_a} + \overline{w(\phi)} - \frac{\partial(\overline{u_a\phi} - \overline{u_a}\overline{\phi})}{\partial x_a}. \tag{4}$$

The last two terms of the right hand side (RHS) of the above equation need closure modeling. In the absence of reaction, the effect of the unresolved scales on the resolved scales manifests only via the last term on the RHS which is usually modeled using a eddy viscosity type model:

$$\overline{u_a\phi} - \overline{u_a}\overline{\phi} = -\mu_T \frac{\partial \overline{\phi}}{\partial x_a}, \tag{5}$$

where the eddy diffusivity coefficient μ_T can be obtained using the dynamic subgrid scale modeling strategy outlined in [3] or the multiple scale elimination scheme [4].

The perils of modeling the filtered reaction term as

$$\overline{w[\phi(\mathbf{x},t)]} = w[\overline{\phi(\mathbf{x},t)}] \tag{6}$$

are well known. Following the procedure used in [2], this term is expressed exactly as

$$\overline{w(\mathbf{x},t)} = \int_{\psi=-\infty}^{\psi=\infty} d\psi w(\psi) f(\psi;\mathbf{x},t), \tag{7}$$

where ψ represents the probability space variable corresponding to the scalar ϕ and the function f is the 'large eddy pdf' (probability density function). If the function f is known, equation (7) can be used to calculate the filtered conversion rate. There are two possible ways of obtaining f. The computationally simpler option, in the same vein as the assumed-pdf approach to turbulent combustion modeling, is to presume the form of $f(\psi;\mathbf{x},t)$ knowing its first few moments at each location [1]. Most assumed pdf's require the specification of

the first two moments: in this case, $\overline{\phi}$ and $\overline{\phi^2}$. The filtered field $\overline{\phi}$ is taken to be known; $\overline{\phi^2}$ may be determined by solving its governing equation:

$$\frac{\partial \overline{\phi^2}}{\partial t} + \overline{u_a}\frac{\partial \overline{\phi^2}}{\partial x_a} = \mu_0 \frac{\partial^2 \overline{\phi^2}}{\partial x_a \partial x_a} - \frac{\partial(\overline{u_a \phi^2} - \overline{u_a}\,\overline{\phi^2})}{\partial x_a} + 2\overline{w(\phi)\phi} - 2\mu_0 \overline{\frac{\partial \phi}{\partial x_a}\frac{\partial \phi}{\partial x_a}}. \tag{8}$$

One of the terms that need modeling in the above equation (8) is the last term on the (RHS) called the filtered scalar dissipation $\mathcal{E}_\phi$. The second, and perhaps the more accurate, option of obtaining the function f is to solve its governing equation [2]. The most important term in the large-eddy pdf governing equation that needs closure modeling is the filtered conditional diffusion. Most of the current models for the filtered conditional diffusion (eg., least mean square estimation, mapping closure methodology) require that the filtered scalar dissipation be known.

It is clear, then, that the role of subgrid scales during mixing, manifesting as the filtered scalar dissipation, is a key process that needs closure modeling. Before attempting its modeling, it is important to understand the basic difference between statistical mean of a quantity denoted by angular brackets (e.g., $\langle \phi^2 \rangle$) and its filtered counterpart represented by a overbar ($\overline{\phi^2}$). The difference is most easily understood in isotropic turbulence where $\langle \phi^2 \rangle$ and $\langle \frac{\partial \phi}{\partial x_a}\frac{\partial \phi}{\partial x_a} \rangle$ are constants in space, but their filtered counterparts exhibit spatial dependence. In Fourier space, the spectrum of the statistical mean is a delta function at zero wavenumber; whereas, the filtered quantity typically has a broad-based spectrum with the highest amplitudes in the small wavenumbers (corresponding to large scales of motion). The lack of a model that can adequately simulate the correct spatial (or, correspondingly, spectral) behavior of the filtered quantity may nullify any advantage that the LES may have over the traditional moment method of calculating mixing and reaction. The filtered scalar dissipation model currently used in literature [1] is an adaptation of the mean scalar dissipation model used in traditional moment methods:

$$\mathcal{E}_\phi = C_\phi \frac{\overline{\phi^2}}{\tau}, \tag{9}$$

where C_ϕ is a constant of order unity and τ is the time scale of turbulence. We will first demonstrate that this model is inadequate for capturing certain important features of filtered scalar dissipation observed in DNS data. We will then proceed to derive a more adequate model expression.

As a first step, in this paper, only inert scalar mixing is considered. In practically all combustion calculations to date, the form of the mean scalar dissipation model used is the same for reacting as well as inert flows. Following suit, even though the current model is developed only for LES of inert scalar mixing, it is recommended for use in reacting cases also. In the discussions so far, G was permitted to be any positive-definite filter. The derivation below is based on a spectral cut-off filter. We speculate that the functional form may be valid for other filters also since the objective of most filters is indeed to separate the large and small scales, even if only approximately.

In Section 2, we perform DNS of passive scalar mixing. We study the DNS data to develop intuition into the behavior of $\overline{\phi^2}$ and $\overline{\frac{\partial \phi}{\partial x_a}\frac{\partial \phi}{\partial x_a}}$. The DNS data is also used to validate some modeling assumptions and ultimately to evaluate the model itself. Section 3 contains model development and validation. We conclude in Section 4 with a summary.

2 Numerical simulations and scalar analysis.

Direct numerical simulations of passive scalar mixing similar to that of Eswaran and Pope [5] are performed. The initially non-premixed scalar field evolves in isotropic turbulence that is held statistically stationary by small wavenumber forcing. The scalar field is initially permitted values of only $+1$ or -1 with equal probability. The calculations are performed on a 64^3 grid, and the Reynolds number based on the Taylor length scale is about 40. The results presented in the paper are for a scalar of Prandtl number unity. Simulations were also performed with non-unity Prandtl numbers and those results are consistent with the presented results. The evolution of the scalar energy (E_ϕ) and dissipation ($D_\phi \equiv k^2 E_\phi(k)$)

spectra are presented in figures 1a and 1b, respectively. As can be seen from the figures, due to the rather modest Reynolds number of the simulation, there is no inertial range or separation of scales. The total number of energetic wavenumbers in a 64^3 simulation with spectral-cut-off de-aliasing is only about 30.

We are primarily interested in modeling the filtered version of the equation

$$\frac{\partial \phi^2}{\partial t} + u_a \frac{\partial \phi^2}{\partial x_a} = \mu_0 \frac{\partial^2 \phi^2}{\partial x_a \partial x_a} - 2\mu_0 \frac{\partial \phi}{\partial x_a} \frac{\partial \phi}{\partial x_a}. \tag{10}$$

Due to the presence of the gradient-squared term (last term on the RHS), the above equation is different from that of a passive scalar. A complete understanding of the spectral behavior of ϕ^2 and the gradient-squared term is important for modeling their filtered counterparts. By writing equation (10) in spectral space and multiplying it through by the complex conjugate, $\phi^{2*}(\mathbf{k})$, we get the spectral budget for ϕ^2-energy:

$$[\frac{\partial}{\partial t} + 2\mu_0 k^2] E_{\phi^2}(\mathbf{k}) = 2T_{\phi^2}(\mathbf{k}) - 4S(\mathbf{k}), \tag{11}$$

where,

$$\begin{aligned} E_{\phi^2}(\mathbf{k}) &= \phi^2(\mathbf{k})\phi^{2*}(\mathbf{k}) \\ S(\mathbf{k}) &= \mu_0 Real[\widehat{\frac{\partial \phi}{\partial x_a} \frac{\partial \phi}{\partial x_a}}(\mathbf{k})\phi^{2*}(\mathbf{k})] = Real[\mathcal{E}_\phi(\mathbf{k})\phi^{2*}(\mathbf{k})]. \end{aligned} \tag{12}$$

In the above equations, superscript * denotes complex conjugate of the quantity and $\hat{}$ indicates Fourier transform. For the sake of convenience, we do not use $\hat{}$ over $\phi(\mathbf{k})$, $\mathcal{E}_\phi(\mathbf{k})$ or $\phi^2(\mathbf{k})$. The second term on the left hand side (LHS) of the above equation (11), $D_{\phi^2}(\mathbf{k}) \equiv 2\mu_0 k^2 E_{\phi^2}(\mathbf{k})$, represents the loss of ϕ^2-energy due to molecular action. The first term on the RHS, $T_{\phi^2}(\mathbf{k})$, represents the net spectral transfer of ϕ^2-energy into wavenumber $\mathbf{k}$ due to the cascading effect of the velocity field. The term $S(\mathbf{k})$ represents ϕ^2-energy transfer into wavenumber $\mathbf{k}$ due to the gradient-squared term.

2.1 Data analysis.

Behavior of $E_{\phi^2}(k)$. The isotropic one-dimensional spectrum $E_{\phi^2}(k)$ calculated from DNS data is given in figure 2a. Most of the ϕ^2 energy is initially present at the large scales or small wavenumbers. With passage of time, larger wavenumbers become more energetic at the expense of the smaller wavenumbers. This transfer of ϕ^2 energy from large to small scales could be due to the effect of the velocity field cascade term ($T_{\phi^2}(k)$) and/or the scalar gradient-squared term ($S(k)$). At the final stages of mixing, as is to be expected, the spectrum decays over the entire wavenumber range.

Behavior of $S(k)$. In physical space, the gradient-squared term always decreases the level of ϕ^2 (equation 10) lowering its spatial mean. This means that, referring to equation (11), the value of $S(\mathbf{k} = 0)$ has to be positive. The behavior of $S(k)$ at other wavenumbers is not clear. By depleting ϕ^2 at different rates at different physical locations, the gradient-squared term may be capable of creating or augmenting spatial fluctuations in the ϕ^2 field. If the gradient-squared term indeed creates or augments ϕ^2 fluctuations at a wavenumber, then it would be a ϕ^2-energy source at that wavenumber. This means that, again referring to equation (11), the value of $S(\mathbf{k})$ at that wavenumber would be negative. In figure 2b, the function $S(k)$ (obtained by summing over all wavenumbers of a given magnitude k) is plotted as a function of $k(> 0)$ at various stages of mixing. Initially, $S(k)$ is negative everywhere indicating that the gradient-squared term acts as a ϕ^2-energy source at all wavenumbers $k > 0$, With time, the magnitude of this energy source decreases. At later times, $S(k)$ is positive at small wavenumbers indicating that it acts as a energy sink at these wavenumbers while still acting as energy source at higher wavenumbers. At the very final stages of mixing, we speculate that $S(k)$ would would be negative everywhere, thereby reducing the fluctuations in ϕ^2 at all scales.

DNS data vs. Moments-method model. The model for LES filtered scalar dissipation given in equation (9), adapted from the moment-method model for the mean scalar dissipation, leads to the following behavior for $S(k)$:

$$S(k) = Real[\frac{C_\phi}{\tau}\phi^2(k)\phi^{2*}(k)] = \frac{C_\phi}{\tau}E_{\phi^2}(k) \geq 0. \tag{13}$$

According to this model, $S(k)$ is always positive, and, hence, a sink of ϕ^2-energy at all wavenumbers and at all times. This, clearly, is inconsistent with the behavior of $S(k)$ observed in the DNS. Even at high Reynolds number, there is no reason why the gradient-squared term cannot transfer ϕ^2-energy from large to small scales and, hence, take negative values at large wavenumbers. Therefore, we conclude that the model for filtered scalar dissipation currently used in literature (equation 9) is inadequate for capturing some important features of scalar mixing.

2.2 Decomposition of scalar dissipation.

If we use the spectral cut-off filter, the scalar and the velocity fields can be decomposed into super and subgrid quantities as follows:

$$\bar{u}_\alpha(\mathbf{k},t) = \begin{cases} u_\alpha(\mathbf{k},t) & \text{if } k \leq \Lambda_c \\ 0 & \text{if } k > \Lambda_c \end{cases} ; \quad u'_\alpha(\mathbf{k},t) = \begin{cases} 0 & \text{if } k \leq \Lambda_c \\ u_\alpha(\mathbf{k},t) & \text{if } k > \Lambda_c \end{cases}$$

and, similarly,

$$\bar{\phi}(\mathbf{k},t) = \begin{cases} \phi(\mathbf{k},t) & \text{if } k < \Lambda_c \text{ ;} \\ 0 & \text{if } k < \Lambda_c. \end{cases} ; \quad \phi'(\mathbf{k},t) = \begin{cases} 0 & \text{if } k < \Lambda_c \\ \phi(\mathbf{k},t) & \text{if } k < \Lambda_c. \end{cases}$$

Here, Λ_c is the wavenumber that separates the resolved and unresolved scales and is typically located in the inertial sub-range. The turbulent velocity field $\mathbf{u}(\mathbf{k},t)$ is determined from the Navier-Stokes equation and the scalar field evolves according to equation (1) with no chemical reaction.

We seek to model the filtered scalar dissipation

$$\mathcal{E}_\phi(\mathbf{x}) = \mu_0 \overline{\frac{\partial\phi}{\partial x_a}\frac{\partial\phi}{\partial x_a}} \tag{14}$$

for the case of spectral cut-off filter. The filtered scalar dissipation can be decomposed into three parts as follows:

$$\begin{aligned} \mathcal{E}_\phi &\equiv \mathcal{E}_\phi^{<<} + \mathcal{E}_\phi^{>>} + \mathcal{E}_\phi^{><} \\ &= \mu_0 \frac{\partial \bar{\phi}}{\partial x_a} \frac{\partial \bar{\phi}}{\partial x_a} + \mu_0 \overline{\frac{\partial \phi'}{\partial x_a} \frac{\partial \phi'}{\partial x_a}} + 2\mu_0 \overline{\frac{\partial \bar{\phi}}{\partial x_a} \frac{\partial \phi'}{\partial x_a}}. \end{aligned} \tag{15}$$

In the above equation (15), the first term on the RHS is the scalar dissipation due to interactions among the resolved scales. This term is closed in the supergrid variables and no modeling is required. The second term on the RHS of (15) represents the scalar dissipation caused by interactions among the unresolved wavenumbers. This term is always positive and requires closure modeling. The third term on the RHS represents the dissipation due to interactions between resolved and unresolved scales. This term, which also needs to be modeled, can be either positive or negative and is responsible for 'backscatter' or energy transfer (of ϕ-energy) from small to large scales. If a sizable spectral gap exists between the resolved and unresolved wavenumbers, this term will be negligible. However, the turbulence spectrum is continuous on either side of the cut-off wavenumber. Analyses of DNS data have demonstrated that interactions of this type play a major role in spectral energy transfer (Zhou and Vahala [6]). Therefore, an accurate description of turbulent mixing must incorporate, as a fundamental building block, this interaction between the resolved and unresolved scales (Rose [7]).

The roles of the three components of dissipation in the spectral budget of ϕ^2-energy are now examined. In particular, the evolutions of $S^{<<}(k)$, $S^{><}(k)$ and $S^{>>}(k)$ -

$$S^{<<}(k) \equiv \mathcal{E}_\phi^{<<}(k)\phi^{2*}(k) \;\; S^{><}(k) \equiv 2\mathcal{E}_\phi^{><}(k)\phi^{2*}(k) \;\; S^{>>}(k) \equiv \mathcal{E}_\phi^{><}(k)\phi^{2*}(k), \tag{16}$$

the three components of $S(k)$ corresponding to the three components of dissipation – are investigated. The results from calculations using DNS data, with $\Lambda_c = 8$, are presented in figure 3. At early times, $S^{<<}(k)$ is much larger than the other two components. At later

times, the three components are of the same order of magnitude. In a typical high Reynolds number turbulent mixing problem of practical interest, we would expect that $S^{<<}(k)$ would be much smaller than the other two components. Two other important observations, from figure 3, which we expect to be valid at high Reynolds number also are: (i) $S^{>>}$ is more important than $S^{><}$ at small supergrid wavenumbers; and, (ii) $S^{><}$ is larger than $S^{>>}$ at the largest supergrid wavenumbers.

Our objective is to construct models for $\mathcal{E}_\phi^{><}$ and $\mathcal{E}_\phi^{>>}$ which will lead to the behavior of $S^{><}(k)$ and $S^{>>}(k)$ consistent with above observations for the supergrid wavenumbers ($k \leq \Lambda_c$).

3 Model development.

In a high Reynolds number scalar mixing problem with adequate scale separation, most of the scalar dissipation, $\mathcal{E}_\phi$(k), is due to $\mathcal{E}_\phi^{>>}(k)$ and it occurs at scales that are much smaller than the length scale corresponding to the cut-off wavenumber, Λ_c. On the contrary, Rose [7] suggests, that most of the contribution towards the back-scatter term, $\mathcal{E}_\phi^{><}(k < \Lambda_c)$, comes from the interactions between the supergrid and the largest subgrid scales, (wavenumbers whose magnitude are of the order Λ_c). In figure 4, we present the contributions of various sub-sets of the subgrid range wavenumbers towards $S^{><}(k)$, calculated using DNS data. It is clear from the figure that most of the contribution indeed is from scales only slightly larger than the cut-off wavenumber. In fact, the contribution from wavenumbers larger than $2\Lambda_c$ is negligible. These observations lead to the following modeling simplifications: only the near subgrid scales contribute towards $\mathcal{E}_\phi^{><}(k)$; and, the only contribution towards $\mathcal{E}_\phi^{>>}(k)$ are from the far subgrid scales. The two components of dissipation are, then, modeled separately employing the assumption of a spectral gap in deriving the model for $\mathcal{E}_\phi^{>>}(k)$ only. To facilitate the implementation of this simplification in our model development, we

subdivide the subgrid wavenumbers into far and near subgrid scales:

$$\phi^{+}(\mathbf{k},t) = \begin{cases} \phi'(\mathbf{k},t) & \text{if } \Lambda_c < k < \Lambda_N \\ 0 & \text{if } k > \Lambda_N. \end{cases} \quad ; \quad \phi^{>}(\mathbf{k},t) = \begin{cases} 0 & \text{if } \Lambda_c < k < \Lambda_N \\ \phi'(\mathbf{k},t) & \text{if } k > \Lambda_N. \end{cases}$$

where, Λ_N ($\leq 2\Lambda_c$) is the cut-off between far and near subgrid scales.

3.1 Model for $\mathcal{E}_{\phi}^{>>}(\mathbf{k})$.

In terms of these new variables we can write

$$\mathcal{E}_{\phi}^{>>} = \mu_0 \overline{\frac{\partial \phi'}{\partial x_a}\frac{\partial \phi'}{\partial x_a}} \approx \mu_0 \overline{\frac{\partial \phi^{>}}{\partial x_a}\frac{\partial \phi^{>}}{\partial x_a}}. \tag{17}$$

In deriving the model for this term, we assume that the scalar field is composed only of the supergrid and far subgrid wavenumbers which are separated by a sizable spectral gap. Clarification of the term 'spectral gap' is called for here. By spectral gap we mean the gap between the supergrid (energy containing scales) and the scales which contribute most towards $\mathcal{E}_{\phi}^{>>}(\mathbf{k})$. The scales of motion that contribute most towards this dissipation are of the order of the Kolmogorov length scale. Therefore, the larger the Reynolds number, the wider is the spectral gap in our definition, and hence, the more valid is the analysis presented below.

It is known from direct interaction approximation [8] and renormalization group theory [9] estimates that, if there is spectral gap, then the effect of the small scales on large scales of motion can be reasonably well accounted for by using a gradient diffusion approximation. Therefore, the total scalar field evolution equation

$$\frac{\partial \phi}{\partial t} + u_a \frac{\partial \phi}{\partial x_a} = \mu_0 \frac{\partial^2 \phi}{\partial x_a \partial x_a}, \tag{18}$$

on elimination of the subgrid scales leads to the following evolution equation for the filtered ϕ field:

$$\frac{\partial \bar{\phi}}{\partial t} + \bar{u}_a \frac{\partial \bar{\phi}}{\partial x_a} = \mu_T \frac{\partial^2 \bar{\phi}}{\partial x_a \partial x_a}. \tag{19}$$

In a high Reynolds number flow the turbulent diffusivity μ_T is much larger than the molecular diffusivity μ_0. In this paper, we are interested in modeling the evolution equation of the filtered ϕ^2 field, whose total field evolves according to

$$\frac{\partial \phi^2}{\partial t} + u_a \frac{\partial \phi^2}{\partial x_a} = \mu_0 \frac{\partial^2 \phi^2}{\partial x_a \partial x_a} - 2\mu_0 \frac{\partial \phi}{\partial x_a} \frac{\partial \phi}{\partial x_a}. \tag{20}$$

We propose that, much in the same way that equation (18) on filtering leads to equation (19), the total ϕ^2 evolution equation (20) would, on filtering, lead to

$$\frac{\partial \overline{\phi^2}}{\partial t} + \bar{u}_a \frac{\partial \overline{\phi^2}}{\partial x_a} = \mu_T \frac{\partial^2 \overline{\phi^2}}{\partial x_a \partial x_a} - 2\mu_T \frac{\partial \bar{\phi}}{\partial x_a} \frac{\partial \bar{\phi}}{\partial x_a}. \tag{21}$$

Comparison of this modeled equation (21) with the exact evolution equation (8) (after setting $w(\phi) = 0$) yields the following. The scalar flux model is

$$-\frac{\partial(\overline{u_a \phi^2} - \overline{u_a}\,\overline{\phi^2})}{\partial x_a} = (\mu_T - \mu_0) \frac{\partial^2 \overline{\phi^2}}{\partial x_a \partial x_a} \approx \mu_T \frac{\partial^2 \overline{\phi^2}}{\partial x_a \partial x_a}. \tag{22}$$

The implied model for filtered dissipation is

$$\mu_0 \overline{\frac{\partial \phi}{\partial x_a} \frac{\partial \phi}{\partial x_a}} \equiv \mu_0 \left(\frac{\partial \bar{\phi}}{\partial x_a} \frac{\partial \bar{\phi}}{\partial x_a} + \overline{\frac{\partial \phi^>}{\partial x_a} \frac{\partial \phi^>}{\partial x_a}} \right) \approx \mu_T \frac{\partial \bar{\phi}}{\partial x_a} \frac{\partial \bar{\phi}}{\partial x_a}. \tag{23}$$

This leads to

$$\mathcal{E}_\phi^{>>} \equiv \mu_0 \overline{\frac{\partial \phi^>}{\partial x_a} \frac{\partial \phi^>}{\partial x_a}} = (\mu_T - \mu_0) \frac{\partial \bar{\phi}}{\partial x_a} \frac{\partial \bar{\phi}}{\partial x_a} \approx \mu_T \frac{\partial \bar{\phi}}{\partial x_a} \frac{\partial \bar{\phi}}{\partial x_a} \tag{24}$$

The eddy diffusivity coefficient μ_T can be obtained using the dynamic subgrid scale modeling strategy outlined in [3] or the multiple scale elimination scheme [4], [7].

As mentioned earlier in this subsection, this model for $\mathcal{E}_\phi^{>>}$ may not be accurate unless there is adequate separation between the supergrid (energy containing) scales and the dissipation scales (of the order of Kolmogorov scales). Hence, the above model cannot be expected to perform well for low Reynolds number mixing problems. With complete cognizance of this fact, we compare the model computations of $S^{>>}(k)$ with DNS data in figures 3, using

$$\frac{\mu_T}{\mu_0} = \frac{\mathcal{E}_\phi^{>>}(k=0)}{\mathcal{E}_\phi^{<<}(k=0)}. \tag{25}$$

In the model calculations, the function $\frac{\partial\overline{\phi}}{\partial x_a}\frac{\partial\overline{\phi}}{\partial x_a}(k)$ is of course taken from DNS data. Except at the final stages of mixing, the model performance is unexpectedly good. The model appears to capture the wavenumber dependence of the $S^{>>}(k)$ reasonably well. The model performance can be expected to be better for higher Reynolds number mixing problems of practical interest.

3.2 Model for $\mathcal{E}_\phi^{><}(\mathbf{k})$.

Many of the shortcomings of LES calculations are generally attributed to the poor, or even lack of, model for the backscatter effect. Derivation of an adequate model for the backscatter dissipation represents a major thrust of this paper. Before we can model the backscatter effect of the near subgrid on the supergrid scales, the effect of the far subgrid on the near subgrid scales must be accounted for. We start with the assumption that the far subgrid affects the near subgrid in the same way that it affects the supergrid scales. In other words, the scope of equation (19) is now extended to include the near subgrid scales as well. Clearly, equation (19) is not as accurate for the near subgrid scales as it is for the supergrid scales, due to the lack of spectral gap between the near and far subgrid scales. Hence, in assuming that the near subgrid scales are also governed by the enhanced diffusivity equation, the backscatter effect between the near and far subgrid is ignored. We argue that, while this neglection may be of concern if we are attempting to model the near subgrid scales, it may be unimportant in the modeling of the interaction between the supergrid and near subgrid scales. Subject to the above simplification, the spectral evolution of the near subgrid scalar field is given by

$$\Big[\frac{\partial}{\partial t} + \mu_T k^2\Big]\phi^+(\mathbf{k},t) = -ik_a \int d^3j u_a(\mathbf{k}-\mathbf{j},t)\phi(\mathbf{j},t), \tag{26}$$

where, $i = \sqrt{-1}$. All of the effects of the far subgrid scales are accounted for by enhancing the diffusivity from μ_0 to μ_T. From this point, the velocity and the scalar fields are considered

as being composed only of the supergrid and near subgrid wavenumbers. Subject to these assumptions we have

$$\mathcal{E}_\phi^{><} = 2\mu_0 \overline{\frac{\partial \bar{\phi}}{\partial x_a} \frac{\partial \phi'}{\partial x_a}} \approx 2\mu_0 \overline{\frac{\partial \bar{\phi}}{\partial x_a} \frac{\partial \phi^+}{\partial x_a}} \tag{27}$$

In spectral space, $\mathcal{E}_\phi^{><}$ can be written as

$$\mathcal{E}_\phi^{><}(\mathbf{k}) = -2\mu_T \langle \int d^3j \; j_a(k-j)_a \overline{\phi}(\mathbf{k}-\mathbf{j}) \phi^+(\mathbf{j}) \rangle. \tag{28}$$

At this stage, one has the option of either deriving a modeled evolution equation for $\mathcal{E}_\phi^{><}$, or seek an algebraic model. For the sake of simplicity, we will restrict ourselves to an algebraic expression for $\mathcal{E}_\phi^{><}$ closed in terms of the supergrid quantities. Most algebraic subgrid scale models – e.g., the Smagorinsky model or the dynamic subgrid scale model for the velocity field – make the implicit assumption that the subgrid scales are in some kind of an equilibrium with the supergrid field, so that no evolution equation is needed for the subgrid scales. We make this equilibrium assumption explicitly and employ its implications to derive the model for $\mathcal{E}_\phi^{><}$.

We start with the assumption that the scalar spectrum of the subgrid scales is in equilibrium with the large scales:

$$\frac{dE_\phi(k)}{dt} = 2T_\phi(k) - 2\mu_T k^2 \phi(k) \phi^*(k) \approx 0, \quad \text{for } \Lambda_c > k > \Lambda_N. \tag{29}$$

In the above, summation is performed over all vector wavenumbers of a given magnitude. (Again following Rose [7], we treat the near subgrid scales as nearly isotropic, even if the supergrid scales are not.) The scalar energy transfer into a wavenumber $\mathbf{k}$ due triadic interactions between the velocity and the scalar fields, denoted by $T_\phi(\mathbf{k})$, has the following form:

$$T_\phi(\mathbf{k}) = Real[-ik_a \int d^3j u_a(\mathbf{k}-\mathbf{j}) \phi(\mathbf{j}) \; \phi^{+*}(\mathbf{k})]. \tag{30}$$

The scalar energy dissipated in wavenumber $\mathbf{k}$ is $D_\phi(\mathbf{k}) = -2\mu_T k^2 \phi(\mathbf{k}) \phi^*(\mathbf{k})$. The simplifying assumption in equation (29) is now verified using DNS data. In figure 5, we plot $T_\phi(k)$ and

$D_\phi(k)$ for the subgrid wavenumbers ($k > \Lambda_c = 12$) at various stages of scalar field decay. At initial times, $T_\phi(k)$ is slightly larger than $D_\phi(k)$ indicating the build up of energy in the near subgrid scales. At later times, due to the decay of the spectra at all wavenumbers, $D_\phi(k)$ is slightly larger than $T_\phi(k)$. However, throughout the mixing process, the difference between $D_\phi(k)$ and $T_\phi(k)$ is much smaller than their absolute magnitude confirming that the simplification in equation (30) is quite reasonable.

Based on the observation that $D_\phi(k) \approx T_\phi(k)$, we suggest that, in an average sense, there is balance at each wavenumber vector: that is,

$$\begin{aligned} D_\phi(\mathbf{k}) &\approx T_\phi(\mathbf{k}) \\ \mu_T k^2 [\phi^+(\mathbf{k})]\phi^{+*}(\mathbf{k}) &\approx Real[-ik_a \int d^3j u_a(\mathbf{k}-\mathbf{j})\phi(\mathbf{j})\phi^{+*}(\mathbf{k})]. \end{aligned} \tag{31}$$

If the above assertion is true, then we must have

$$\phi^+(\mathbf{k},t) = \frac{1}{\mu_T k^2}[-ik_a \int d^3j u_a(\mathbf{k}-\mathbf{j},t)\phi(\mathbf{j},t) + C_0\tilde{\phi}^+(\mathbf{k},t)], \tag{32}$$

where, C_0 is a constant and $\tilde{\phi}^+(\mathbf{k})$ is such that

$$\tilde{\phi}^+(\mathbf{k},t)\phi^{+*}(\mathbf{k},t) = 0. \tag{33}$$

Substituting equation (32) into the expression for $\mathcal{E}_\phi^{><}(\mathbf{k})$ in equation (28) we get

$$\begin{aligned} \mathcal{E}_\phi^{><}(\mathbf{k}) &= -2\mu_T \langle \int d^3j\, j_a(k-j)_a \overline{\phi}(\mathbf{k}-\mathbf{j}) \frac{1}{\mu_T j^2}[-ij_b \int d^3j' u_b(\mathbf{j}-\mathbf{j}')\phi(\mathbf{j}') + C_0\tilde{\phi}^+(\mathbf{j})] \rangle \\ &= 2\langle \int\int d^3j d^3j' (\frac{ij_b}{j^2}) j_a(k-j)_a \overline{\phi}(\mathbf{k}-\mathbf{j}) u_b(\mathbf{j}-\mathbf{j}')\phi(\mathbf{j}') \rangle \\ &\quad -2C_0\langle \int d^3j j_a(k-j)_a (\frac{1}{j^2}) \overline{\phi}(\mathbf{k}-\mathbf{j})\tilde{\phi}^+(\mathbf{j}) \rangle. \end{aligned} \tag{34}$$

In the above equation, the integration over j is restricted to subgrid wavenumbers, whereas, the integration over j' is over all wavenumbers. Considering that the subgrid now consists only of a narrow band of scales, we propose that, to leading order,

$$\begin{aligned} \langle \int\int d^3j d^3j' j_a(k-j)_a (\frac{ij_b}{j^2}) & \quad \overline{\phi}(\mathbf{k}-\mathbf{j}) u_b(\mathbf{j}-\mathbf{j}')\phi(\mathbf{j}') \rangle \\ &\approx \langle \int\int d^3j d^3j' j_a(k-j)_a (\frac{ij_b}{j^2}) \overline{\phi}(\mathbf{k}-\mathbf{j}) \overline{u}_b(\mathbf{j}-\mathbf{j}') \overline{\phi}(\mathbf{j}') \rangle. \end{aligned} \tag{35}$$

After this truncation to the leading order term, the only remaining unclosed term in the model for $\mathcal{E}_\phi^{><}$ is the one containing $\tilde{\phi}^+$. Calculations of this term from DNS data (result not shown) appear to indicate that it is not small in magnitude compared to the other term (equation 32) in the model expression for $\mathcal{E}_\phi^{><}$. However, we know from equation (33) that this term does not affect the level of the scalar energy. Since our main interest in $\mathcal{E}_\phi^{><}$ is to be able to calculate the level of scalar energy of the supergrid ($\overline{\phi^2}$) correctly, we suggest that the term containing $\tilde{\phi}^+$ be dropped from the model expression. In other words, we suggest that exclusion of this unclosed term would still lead to the correct behavior of the ultimately important quantity $S^{><}(k)$ (see equation 16 for definition), even if the behavior of $\mathcal{E}_\phi^{><}(k)$ itself may not be quite correct. The extent of validity of this exclusion will be borne out when the model calculations of $S^{><}(k)$ are compared against DNS data.

The expression for $\mathcal{E}_\phi^{><}(\mathbf{k})$ (equation 34) can now be approximated as (the angular brackets indicating averaging are dropped because only the supergrid quantities survive our simplification)

$$\mathcal{E}_\phi^{><}(\mathbf{k}) \approx 2 \int d^3j d^3j' (k-j)_a j_a \left(\frac{ij_b}{j^2}\right) \bar{u}_b(\mathbf{j}-\mathbf{j}',t)\bar{\phi}(\mathbf{j}',t)\bar{\phi}(\mathbf{k}-\mathbf{j},t). \tag{36}$$

The above equation represents a closure model for the backscatter dissipation in spectral space. Most of the LES computations are performed in physical space, and, therefore, a closure model in physical space would be very useful. Inverse Fourier transformation of equation (36) would lead to an expression that involves Greens integral over space, and, hence, not local in space. The non-locality of the closure model for $\mathcal{E}_\phi^{><}$ will preclude it from being useful in LES computations of high Reynolds number flows of complex geometry.

A model local that is local in physical space can be obtained if we assume that the contribution towards $\mathcal{E}_\phi^{><}$ comes only from a thin shell of subgrid wavenumbers, an approximation that is justified by the finding in figure 4. Then, in equation (36) we can set $|j| \approx \Lambda_c$ (recall

that the dummy wavenumber j is restricted to near subgrid scales), leading to

$$\mathcal{E}_\phi^{><}(\mathbf{k}) \approx \frac{2}{\Lambda_c^2}\int d^3j d^3j'(k-j)_a j_a (ij_b)\bar{u}_b(\mathbf{j}-\mathbf{j}',t)\bar{\phi}(\mathbf{j}',t)\bar{\phi}(\mathbf{k}-\mathbf{j},t). \tag{37}$$

By performing a convolution integral over j' (which is over the entire wavenumber domain), we get

$$\begin{aligned}\mathcal{E}_\phi^{><}(\mathbf{k}) &= \frac{2}{\Lambda_c^2}\int d^3j (k-j)_a j_a (ij_b)[\widehat{\bar{u}_b\bar{\phi}}](\mathbf{j},t)\bar{\phi}(\mathbf{k}-\mathbf{j},t) \\ &= -\frac{2}{\Lambda_c^2}\int d^3j \frac{\widehat{\partial^2\bar{u}_b\bar{\phi}}}{\partial x_a \partial x_b}(\mathbf{j},t)\frac{\widehat{\partial\bar{\phi}}}{\partial x_a}(\mathbf{k}-\mathbf{j},t).\end{aligned} \tag{38}$$

The integration over j (subgrid scales only) can be split into two parts

$$\begin{aligned}\int_{subgrid} d^3j \frac{\widehat{\partial^2\bar{u}_b\bar{\phi}}}{\partial x_a \partial x_b}(\mathbf{j},t)\frac{\widehat{\partial\bar{\phi}}}{\partial x_a}(\mathbf{k}-\mathbf{j},t) &= \int_{total} d^3j \frac{\widehat{\partial^2\bar{u}_b\bar{\phi}}}{\partial x_a \partial x_b}(\mathbf{j},t)\frac{\widehat{\partial\bar{\phi}}}{\partial x_a}(\mathbf{k}-\mathbf{j},t) \\ &\quad - \int_{supergrid} d^3j \frac{\widehat{\partial^2\bar{u}_b\bar{\phi}}}{\partial x_a \partial x_b}(\mathbf{j},t)\frac{\widehat{\partial\bar{\phi}}}{\partial x_a}(\mathbf{k}-\mathbf{j},t)\end{aligned} \tag{39}$$

Each integration can now be separately evaluated:

$$\int_{total} d^3j \frac{\widehat{\partial^2\bar{u}_b\bar{\phi}}}{\partial x_a \partial x_b}(\mathbf{j},t)\frac{\widehat{\partial\bar{\phi}}}{\partial x_a}(\mathbf{k}-\mathbf{j},t) = [\frac{\partial^2\bar{u}_b\bar{\phi}}{\partial x_a \partial x_b}\frac{\partial\bar{\phi}}{\partial x_a}](\mathbf{k}) \tag{40}$$

$$\int_{supergrid} d^3j \frac{\widehat{\partial^2\bar{u}_b\bar{\phi}}}{\partial x_a \partial x_b}(\mathbf{j},t)\frac{\widehat{\partial\bar{\phi}}}{\partial x_a}(\mathbf{k}-\mathbf{j},t) = \int_{total} d^3j \overline{\frac{\widehat{\partial^2\bar{u}_b\bar{\phi}}}{\partial x_a \partial x_b}}(\mathbf{j},t)\frac{\widehat{\partial\bar{\phi}}}{\partial x_a}(\mathbf{k}-\mathbf{j},t) = [\overline{\frac{\widehat{\partial^2\bar{u}_b\bar{\phi}}}{\partial x_a \partial x_b}}\frac{\partial\bar{\phi}}{\partial x_a}](\mathbf{k},t).$$

Therefore, the exact inverse transform of equation (38) yields,

$$\mathcal{E}_\phi^{><}(x) = -\frac{2}{\Lambda_c^2}\frac{\partial\bar{\phi}}{\partial x_a}[\frac{\partial^2\bar{u}_b\bar{\phi}}{\partial x_a \partial x_b} - \overline{\frac{\partial^2\bar{u}_b\bar{\phi}}{\partial x_a \partial x_b}}]. \tag{41}$$

The parameter Λ_c can be expressed in terms of the mechanical dissipation rate ($\mathcal{E}$) and the kinetic energy (K) of the subgrid scales (e.g., Rubinstein and Barton [10], Zhou et al. [11]):

$$\Lambda_c = \frac{\mathcal{E}}{K^{3/2}}(3C_k/2)^{3/2}, \tag{42}$$

where C_k is the Kolmogorov constant. To obtain the relations in equation (42), the velocity field is assumed to be stationary and the small scale autocorrelation is taken to be determined

by the Kolmogorov spectrum. After substituting Λ_c from equation (42), the model expression for $\mathcal{E}_\phi^{><}$ in terms of the subgrid turbulent velocity field variables is given by

$$\mathcal{E}_\phi^{><}(x) = -C_\phi^{><} \frac{K^3}{\mathcal{E}^2} \frac{\partial \bar{\phi}}{\partial x_a} [\frac{\partial^2 \bar{u}_b \bar{\phi}}{\partial x_a \partial x_b} - \overline{\frac{\partial^2 \bar{u}_b \bar{\phi}}{\partial x_a \partial x_b}}]. \tag{43}$$

where $C_\phi^{><}$ is independent of the wavenumber.

We now compare our model against DNS data. We reiterate that the main emphasis of the modeling effort is to be able to calculate the correct spectral behavior of the supergrid component of ϕ^2 which evolves according to equation (8). To examine if the proposed model accomplishes the stated objective, we compare the model calculation with DNS for the quantity $S^{><}(k) \equiv \mathcal{E}_\phi^{><} \phi^{2*}(k)$ in figure 6. The comparison is performed at four different stages of the mixing process with $\Lambda_c = 12$; $C_\phi^{><}$ is taken to be that numerical value which gives the best agreement at each time. The model agrees very well with DNS data, especially at early times. As required, the model appears to capture the wavenumber dependence of $S(k)$ very well. The modeling is complete except for the specification of $C_\phi^{><}$ which determines only the overall level of $S(k)$ and not its spectral character. The determination of $C_\phi^{><}$ is deferred to a future effort.

4 Conclusion.

In this paper, we first study the behavior of filtered scalar dissipation – arising in LES modeling of turbulent scalar mixing – with the help of DNS data. Then, we employ the insight gained to develop a model expression for the filtered scalar dissipation. It is found that its accurate modeling requires that two physical phenomena be accounted for: (i) the dissipation due to interaction among the subgrid scales, denoted by $\mathcal{E}_\phi^{>>}$; and, (ii) the dissipation due to the interaction between the resolved and unresolved scales, given by $\mathcal{E}_\phi^{><}$.

Arguing that the dominant contribution towards $\mathcal{E}_\phi^{>>}$ comes from the interaction among far-field subgrid wavenumbers, we introduce an artificial spectral gap in the derivation of the

model for this term. The model for $\mathcal{E}_\phi^{>>}$ turns out to be an enhanced molecular diffusion type term, as it should be in the distant interaction approximation limit. Although the assumptions leading to this model are valid only for high Reynolds number turbulent mixing, comparison with low Reynolds number DNS data shows surprisingly adequate performance by the model.

It is also demonstrated using DNS data that most contribution to the 'backscatter'-dissipation, $\mathcal{E}_\phi^{><}$, comes from a narrow band of subgrid wavenumbers only slightly larger than the largest supergrid wavenumber. After establishing that the scalar spectrum of this near subgrid wavenumber band is in quasi-equilibrium with the large (supergrid) scales, we derive the model for $\mathcal{E}_\phi^{><}$ in its most accurate form in the spectral space. Inverse transform into physical space leads to a non-local model, which in large scale LES calculations, could lead to excessive computational requirements. A less accurate, but computationally more feasible, model for this term that is local in physical space is derived by assuming that only a thin shell of wavenumbers contribute towards the 'backscatter'. Comparison of this model with DNS data shows good agreement.

The present model appears to be a clear improvement over the previously used model for filtered scalar dissipation. The previous model, which is a literal extension of the model for the statistical average of scalar dissipation used in moment methods, makes no use of the additional information about the supergrid scalar field available in a LES computation. The present model makes use of the additional supergrid scalar field information available, leading to a more accurate model. Owing to the reasonably sound theoretical foundation of the new model, coupled with its demonstrated ability to capture important features of DNS mixing data, we expect that the model derived in this paper would be very useful for accurate LES computations of scalar mixing and reaction.

References

[1] Adumitroaie, V., Frankel, S. H., Madnia, C. K., and Givi, P., *Large eddy simulation and direct numerical simulation of high speed turbulent reacting flows.* State University of New York report (1993), Turbulence Research Laboratory, SUNY at Buffalo, Buffalo, New York 14260.

[2] Gao, F., and O'Brien, E. E., *A large-eddy simulation scheme for turbulent reacting flows.* Phys. Fluids A, **5** (6), 1282 (1993).

[3] Moin, P., Squires, K., Cabot, W., and Lee, S., *A dynamic subgrid-scale model for compressible turbulence and scalar transport.* Phys. Fluids A, **3**, 2746 (1991).

[4] Zhou,Y., Vahala, G., *Renormalization-group estimates of transport coefficients in the advection of a passive scalar by incompressible turbulence.* Phys. Rev. E, **48**, 4387 (1993).

[5] Eswaran, V., and Pope, S. B., *A Direct numerical simulations of the mixing of a passive scalar.* Phys. Fluids, **31**, 506 - 520 (1988).

[6] Zhou, Y., and Vahala, G., *Reformulation of recursive renormalization group based subgrid modeling of turbulence.* Phys. Rev. E, **47**, 2503 (1993).

[7] Rose, H. A., *Eddy diffusivity, eddy noise, and subgrid-scale modeling.* J. Fluid Mech., **81**, 719 (1977).

[8] Kraichnan, R. H., *An interpretation of Yakhot-Orszay turbulence theory.* Phys. Fluids, **30**, 2400 (1987).

[9] Zhou, Y., Vahala, G., *Renormalization group theory for the eddy viscosity in subgrid modeling.* Phys. Rev. A, **37**, 2590 (1988).

[10] Rubinstein, R., and Barton, J. M., *Nonlinear Reynolds stress model and the renormalization group.* Phys. Fluids A, **2**, 1472 (1990).

[11] Zhou,Y., Vahala, G., and Thangam, S., *Development of a recursive RNG based turbulence model.* Phys. Rev. E, **49**, 5195 (1994).

Fig. 1a: Scalar Spectrum

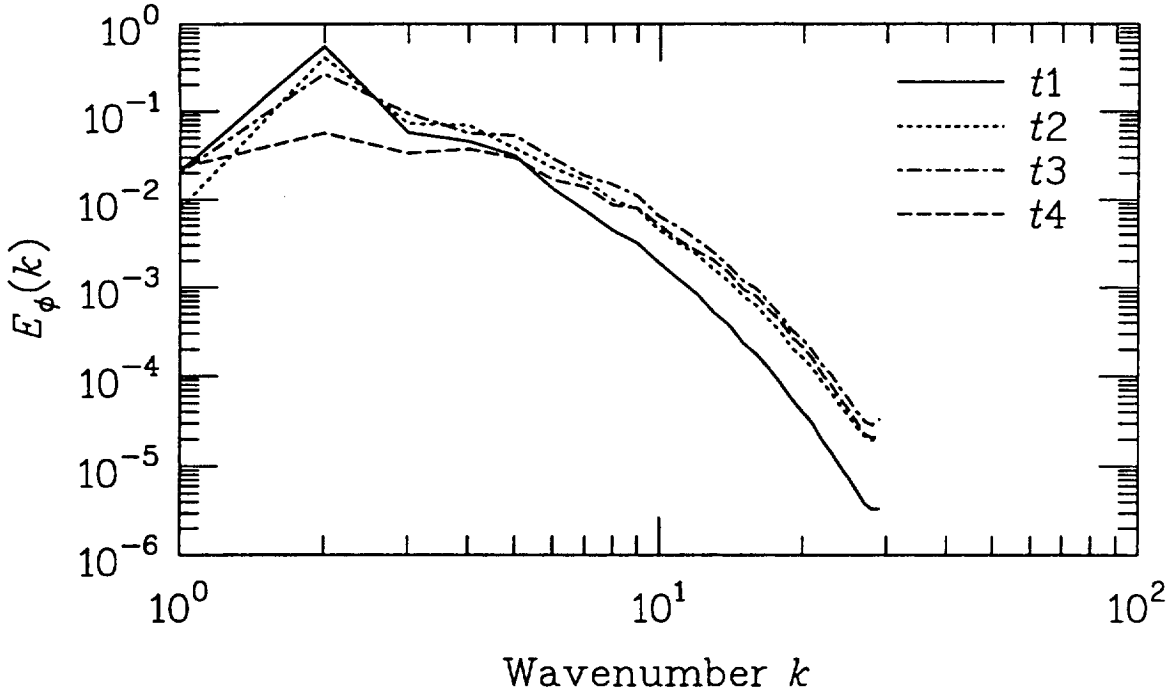

Fig. 1b: Dissipation Spectrum

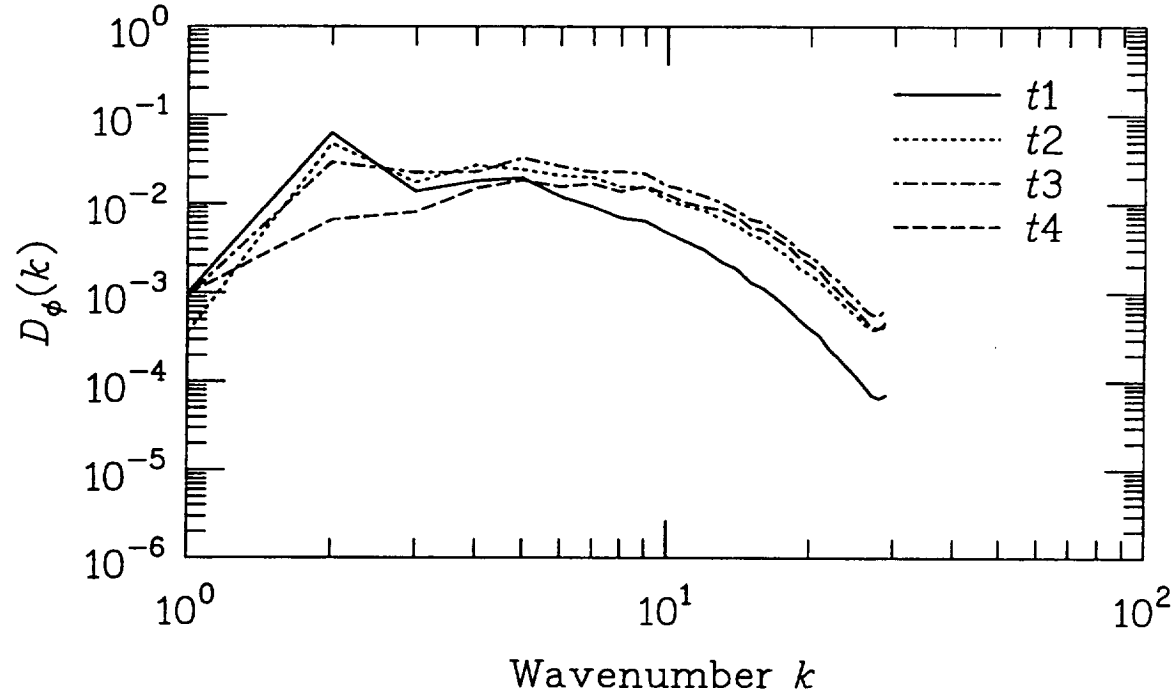

Figure 1: Evolution of scalar spectra calculated from DNS data: (a) Energy spectrum; (b) Dissipation spectrum. Times: t1 = 1.25 τ_η; t2 = 2.5 τ_η; t3 = 3.5 τ_η; and t4 = 5.25 τ_η, where the Kolmogorov time scale of turbulence $\tau_\eta \approx 0.1$.

Fig. 2a

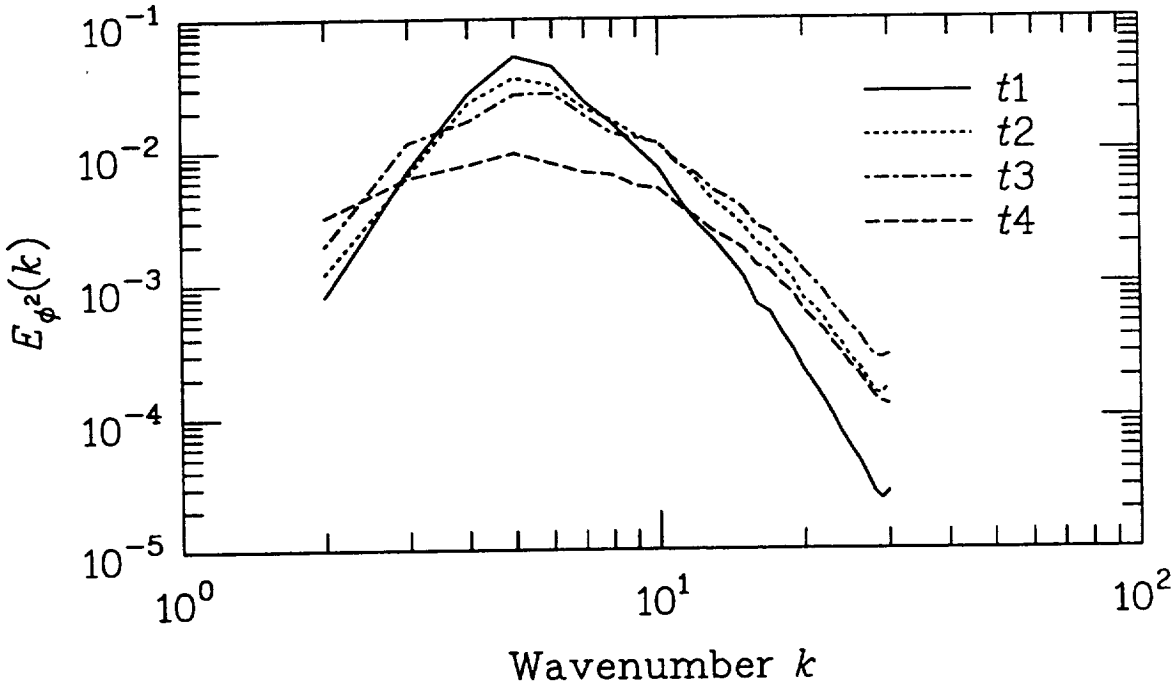

Fig. 2b

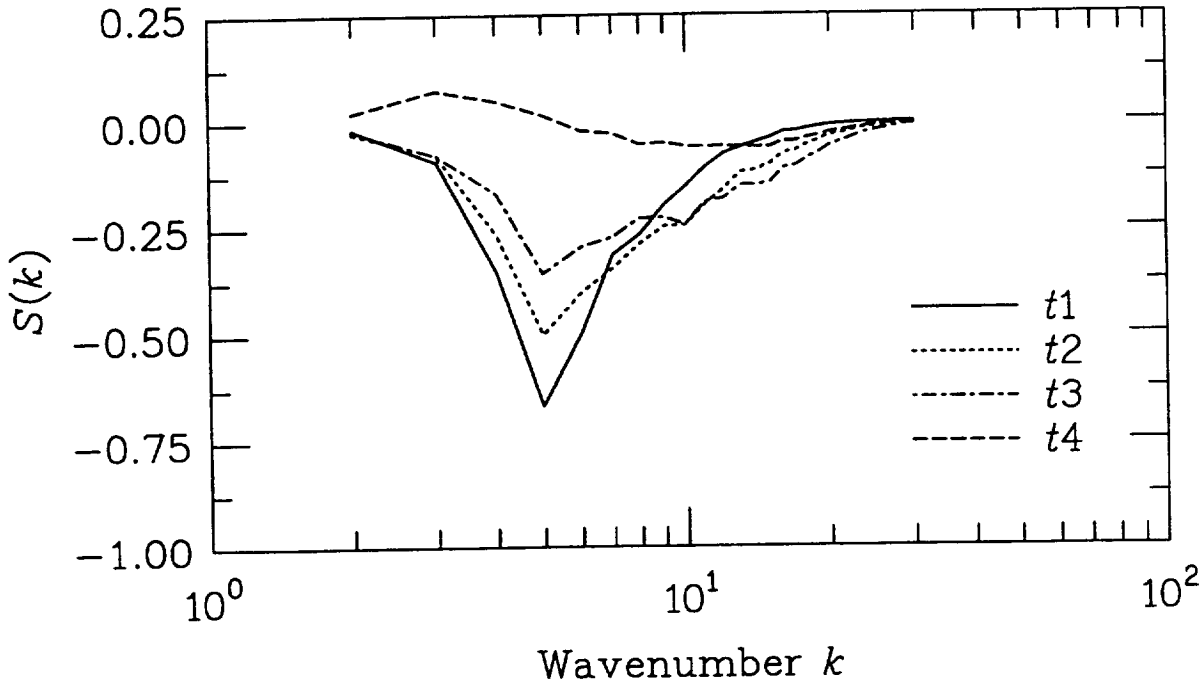

Figure 2: (a) Evolution of the energy spectrum of ϕ^2. (b) Evolution of $S(k) = \text{Real}[\mathcal{E}_\phi(k)\phi^{2*}(k)]$. Times same as given in figure 1.

Fig. 3a: Time t1

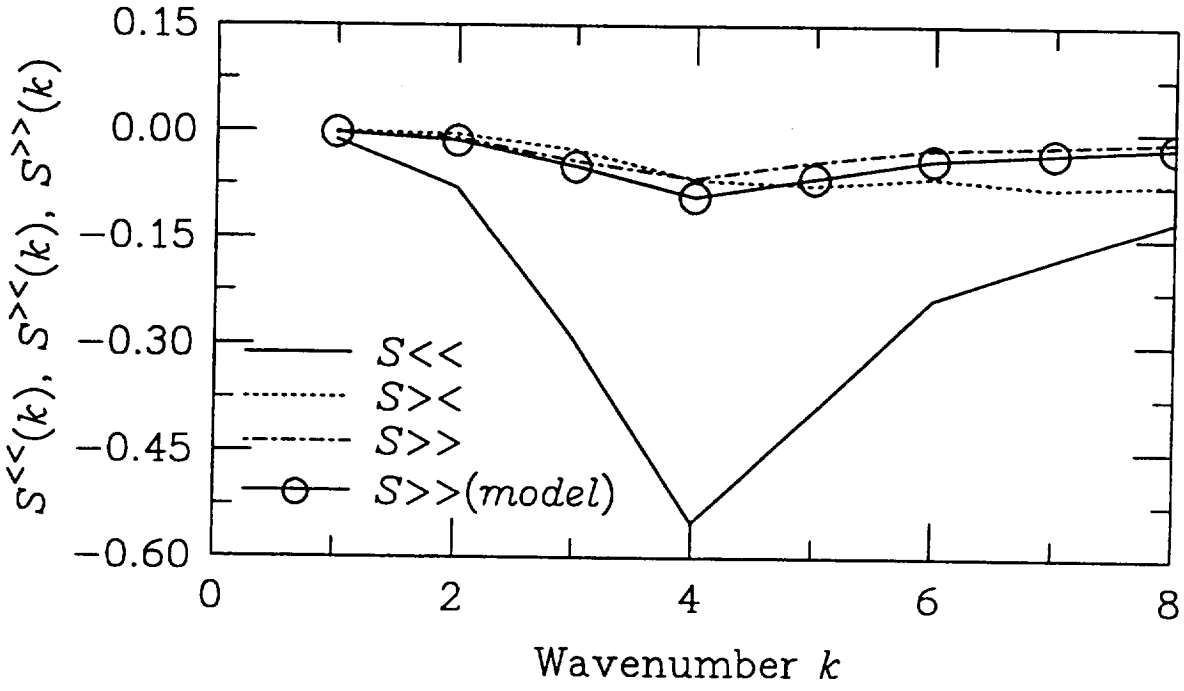

Fig. 3b: Time t2

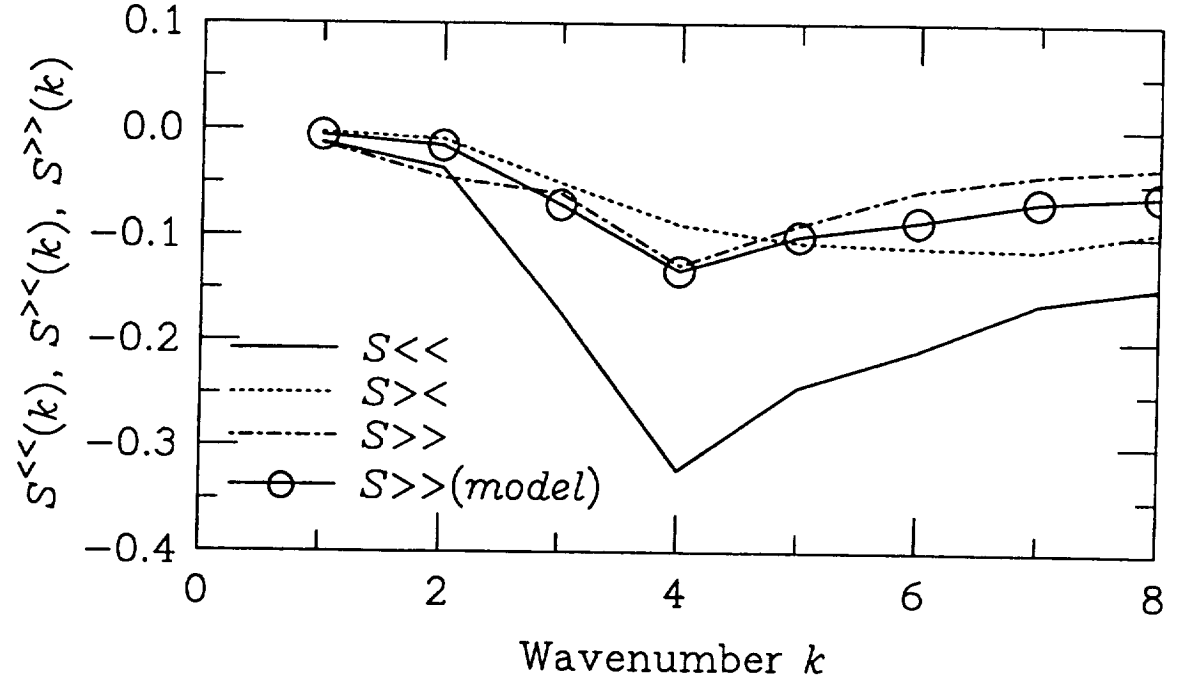

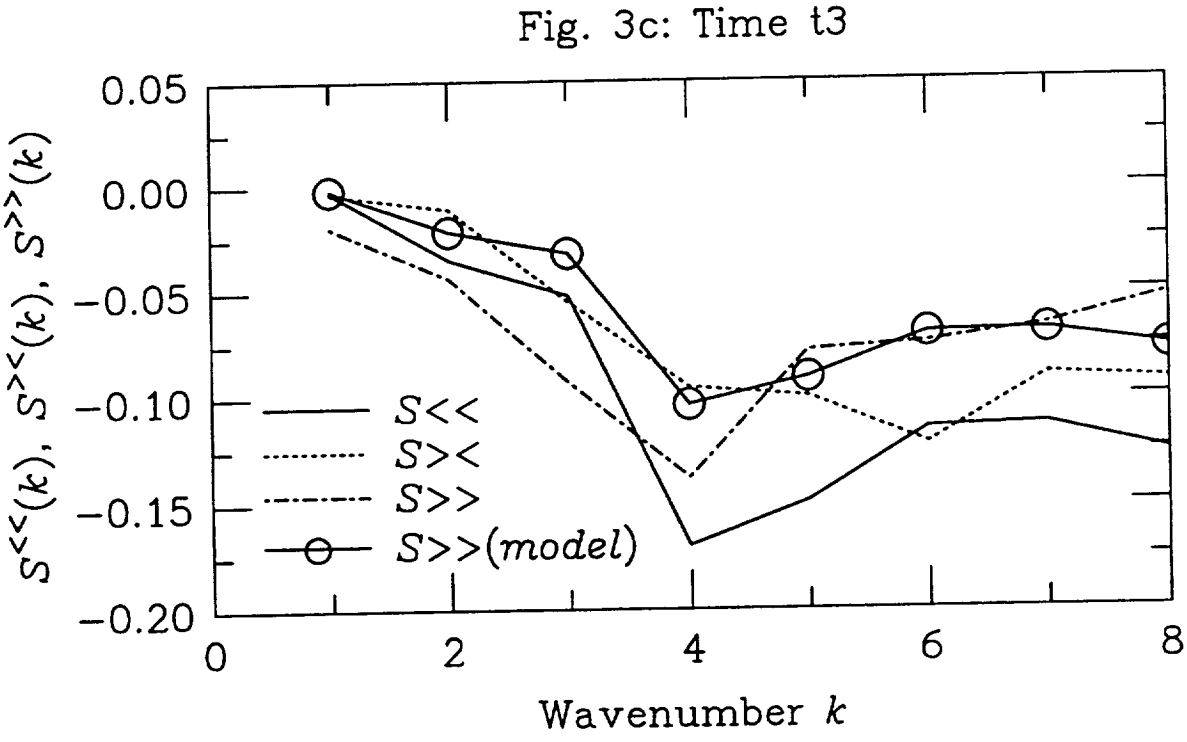

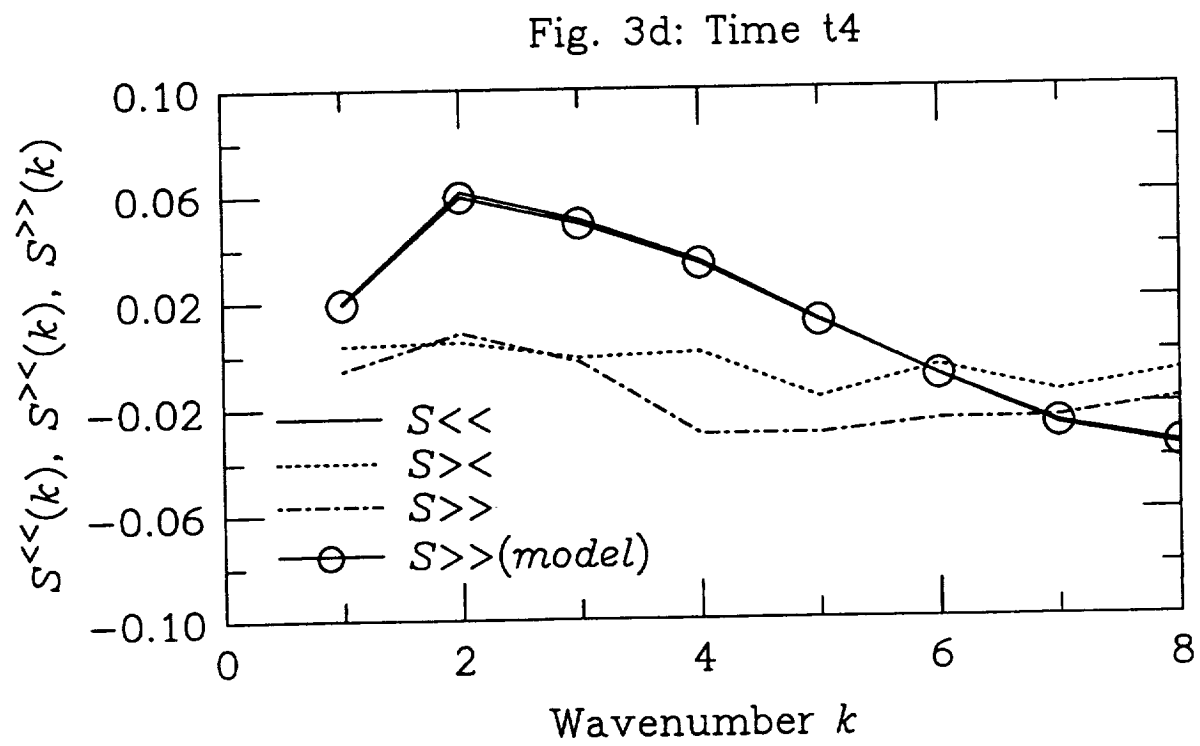

Figure 3: Evolution of the various components of $S(k)$ calculated from DNS data. Evolution of $S^{>>}(k)$ as computed by the enhanced diffusion model is also presented. Cut-off wavenumber $\Lambda_c = 8$. Times same as given in figure 1.

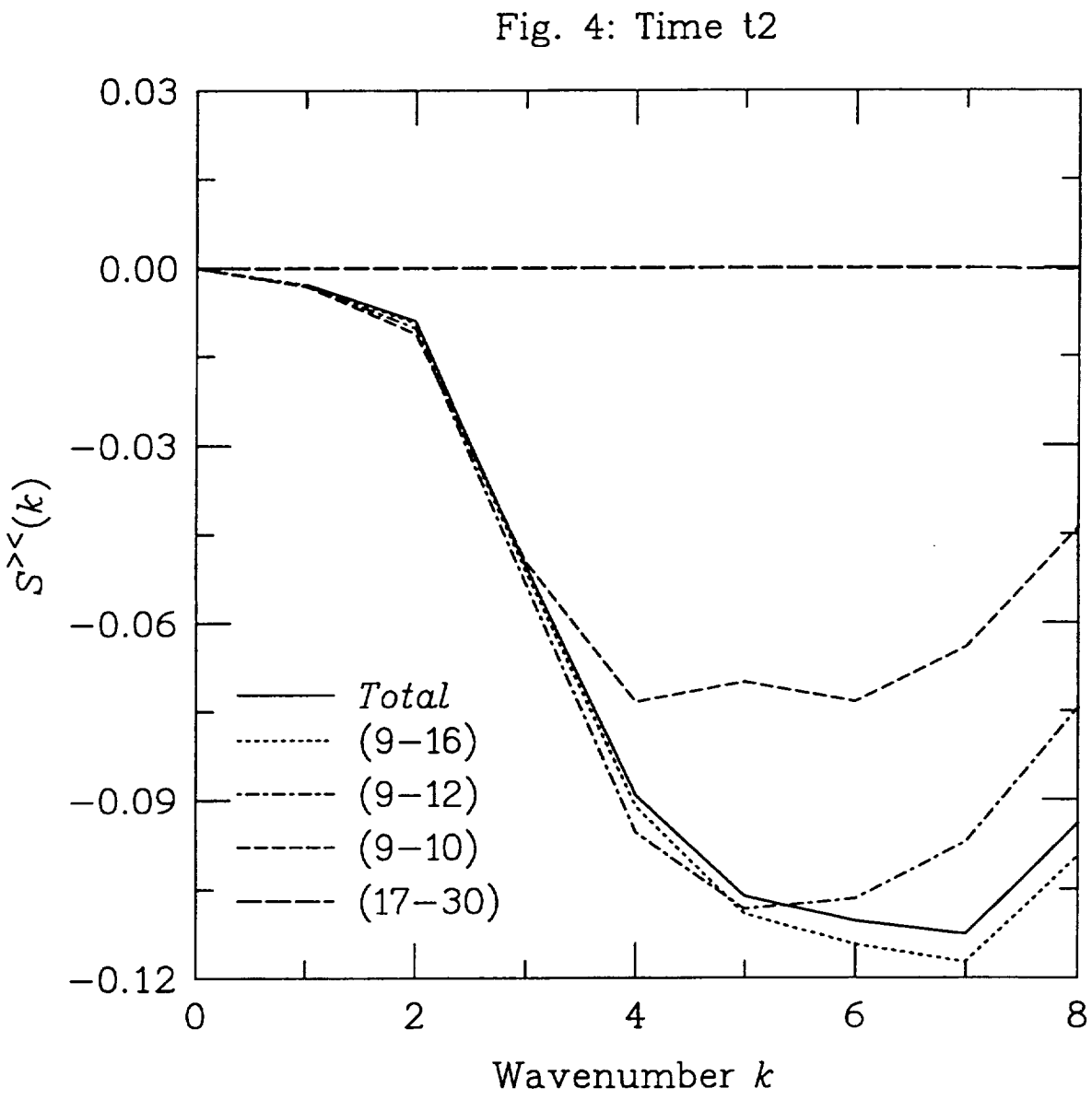

Figure 4: Contribution of various wavenumber bands towards $S^{><}(k)$ calculated from DNS data. The results shown are for time t2 with $\Lambda_c = 8$.

Fig. 5a: Time t1

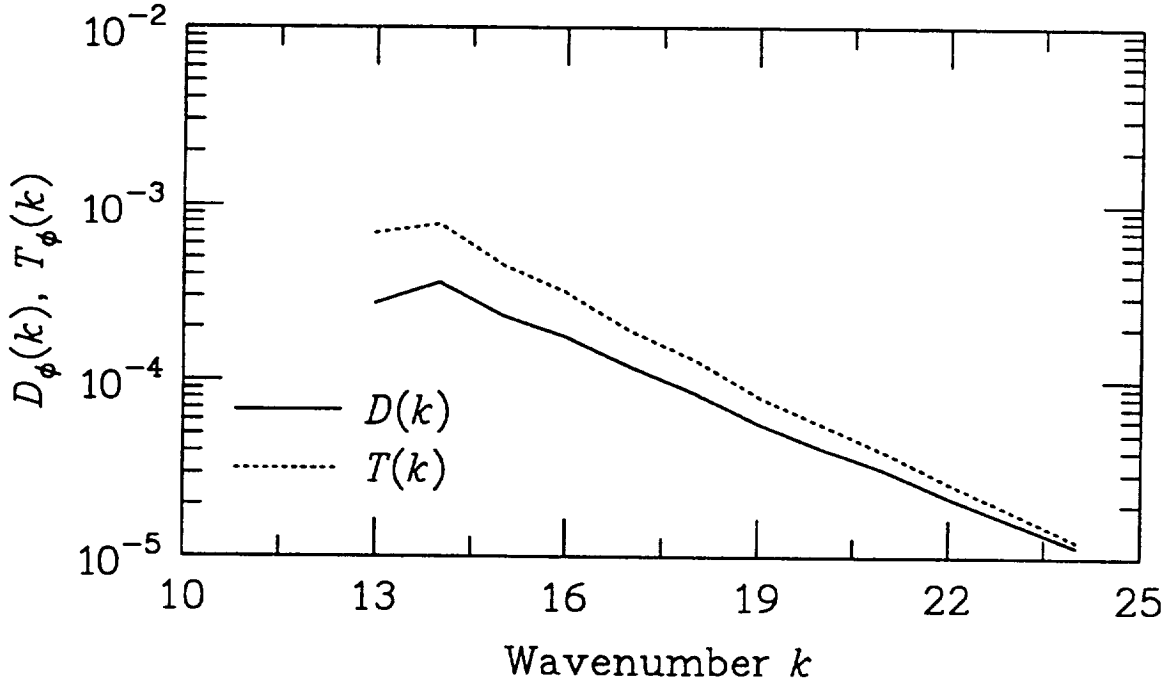

Fig. 5b: Time t2

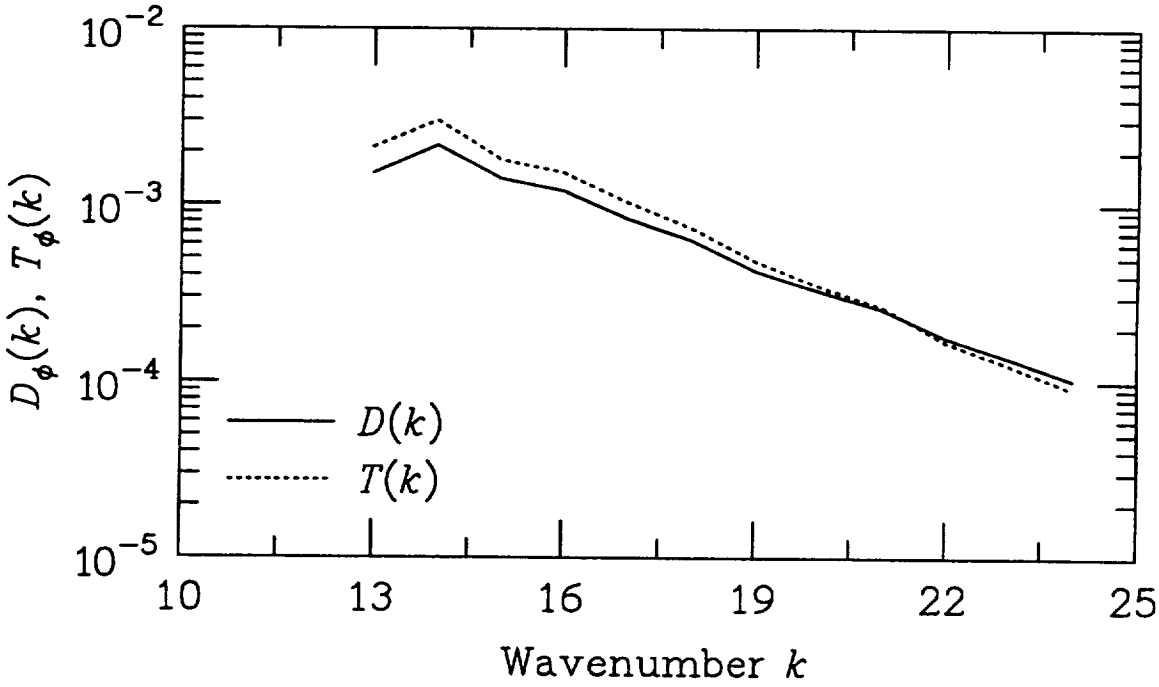

Fig. 5c: Time t3

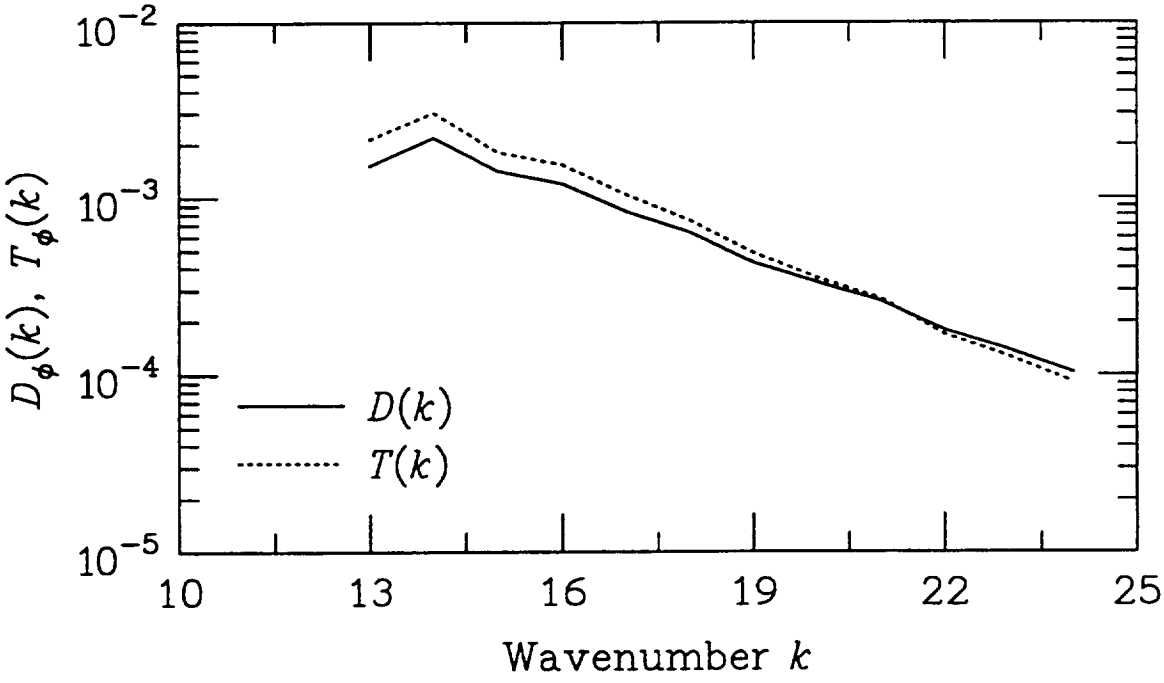

Fig. 5d: Time t4

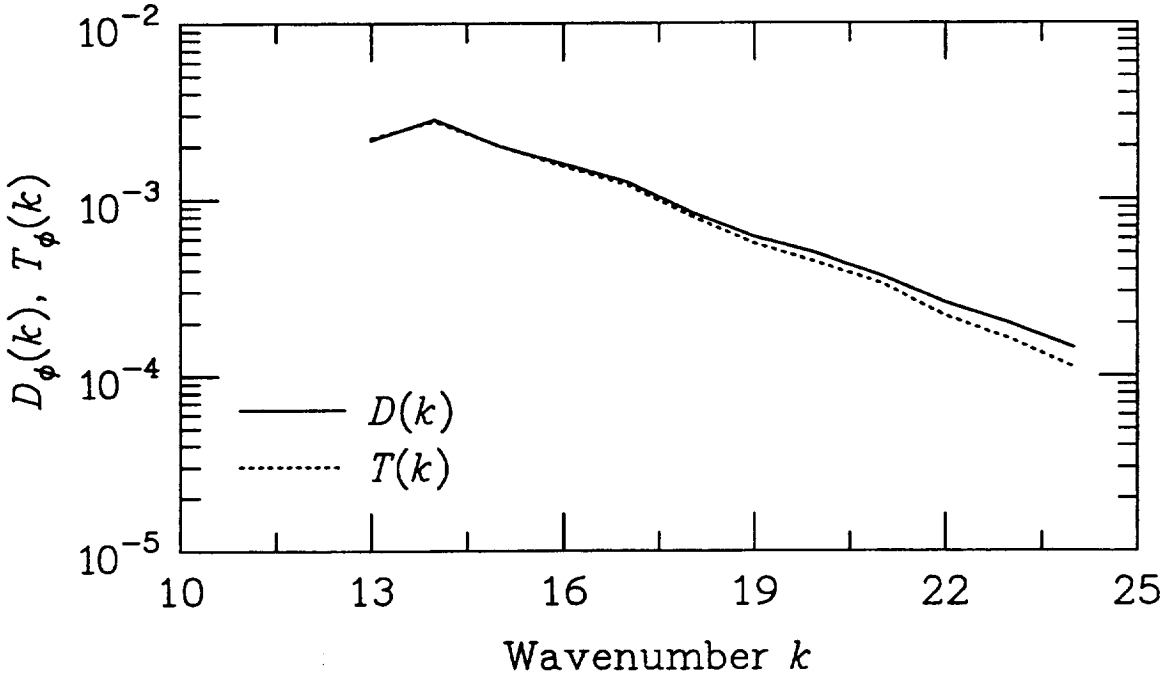

Figure 5: Evolution of D(k) and T(k) of the scalar spectrum evolution equation (DNS data). Times same as given in figure 1.

Fig. 6a: Time t1

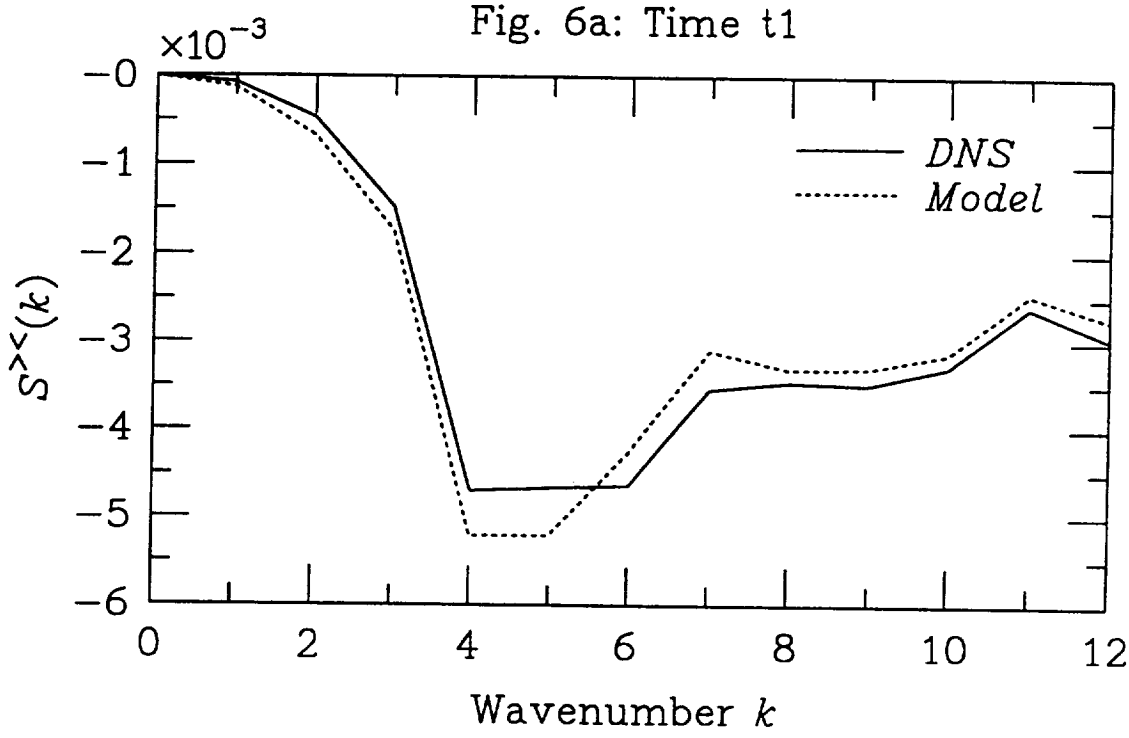

Fig. 6b: Time t2

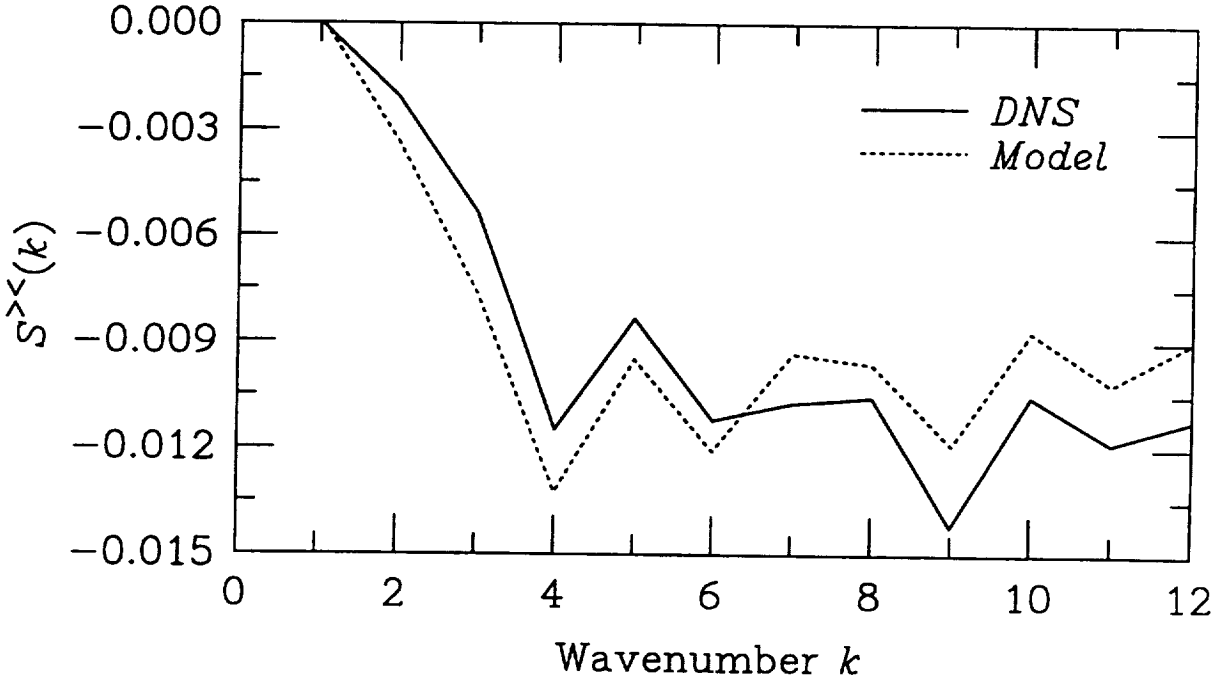

Fig. 6c: Time t3

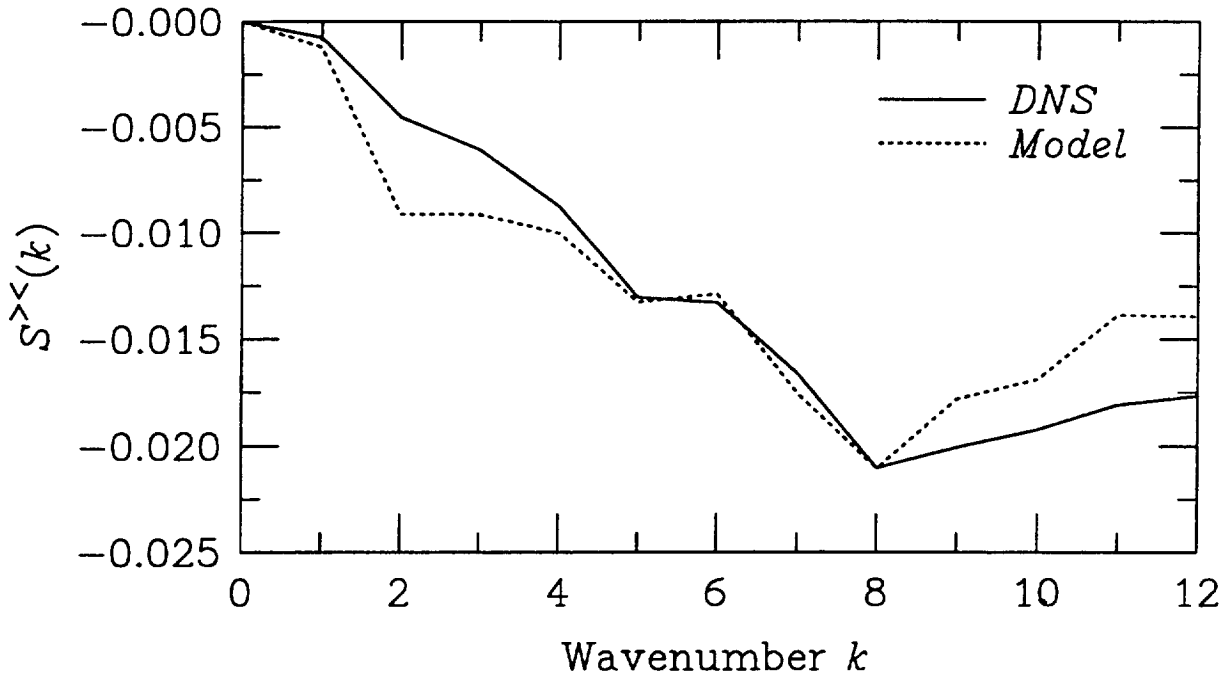

Fig. 6d: Time t4

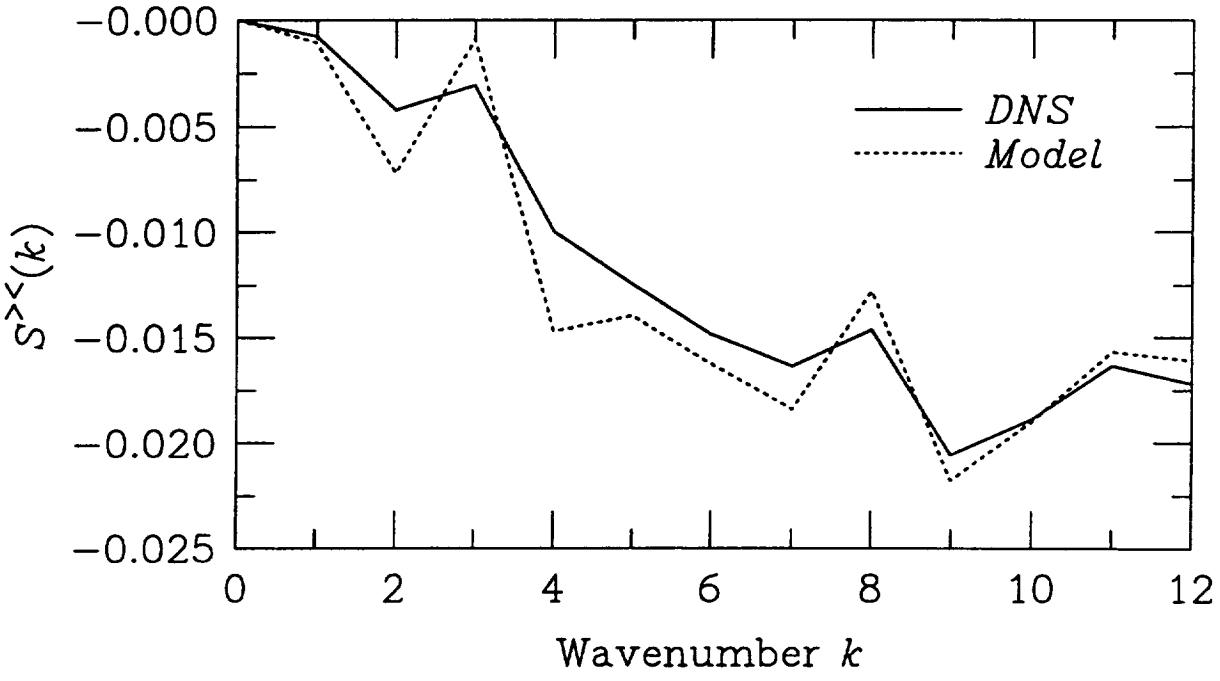

Figure 6: Comparison between DNS data and model for $S^{><}(k)$. The cut-off wavenumber $\Lambda_c = 12$. Times of comparison are the same as given in figure 1.

REPORT DOCUMENTATION PAGE

Form Approved
OMB No. 0704-0188

1. AGENCY USE ONLY *(Leave blank)*

2. REPORT DATE
May 1995

3. REPORT TYPE AND DATES COVERED
Contractor Report

4. TITLE AND SUBTITLE
ANALYSIS AND MODELING OF SUBGRID SCALAR MIXING USING NUMERICAL DATA

5. FUNDING NUMBERS
C NAS1-19480
WU 505-90-52-01

6. AUTHOR(S)
Sharath S. Girimaji
Ye Zhou

7. PERFORMING ORGANIZATION NAME(S) AND ADDRESS(ES)
Institute for Computer Applications in Science
and Engineering
Mail Stop 132C, NASA Langley Research Center
Hampton, VA 23681-0001

8. PERFORMING ORGANIZATION REPORT NUMBER
ICASE Report No. 95-44

9. SPONSORING/MONITORING AGENCY NAME(S) AND ADDRESS(ES)
National Aeronautics and Space Administration
Langley Research Center
Hampton, VA 23681-0001

10. SPONSORING/MONITORING AGENCY REPORT NUMBER
NASA CR-198169
ICASE Report No. 95-44

11. SUPPLEMENTARY NOTES
Langley Technical Monitor: Dennis M. Bushnell
Final Report
To be submitted to Physics of Fluids

12a. DISTRIBUTION/AVAILABILITY STATEMENT
Unclassified–Unlimited

Subject Category 34

12b. DISTRIBUTION CODE

13. ABSTRACT *(Maximum 200 words)*

Direct numerical simulations (DNS) of passive scalar mixing in isotropic turbulence is used to study, analyze and, subsequently, model the role of small (subgrid) scales in the mixing process. In particular, we attempt to model the dissipation of the large scale (supergrid) scalar fluctuations caused by the subgrid scales by decomposing it into two parts: (i) the effect due to the interaction among the subgrid scales, $\mathcal{E}_\phi^{>>}$; and, (ii) the effect due to interaction between the supergrid and the subgrid scales, $\mathcal{E}_\phi^{><}$. Model comparison with DNS data shows good agreement. This model is expected to be useful in the large eddy simulations of scalar mixing and reaction.

14. SUBJECT TERMS
scalar mixing; LES modeling of mixing; turbulence modeling

15. NUMBER OF PAGES
31

16. PRICE CODE
A03

17. SECURITY CLASSIFICATION OF REPORT	18. SECURITY CLASSIFICATION OF THIS PAGE	19. SECURITY CLASSIFICATION OF ABSTRACT	20. LIMITATION OF ABSTRACT
Unclassified	Unclassified		